1D-Polyoxometalate-Based Composite Compounds − Design, Synthesis, Crystal Structures, and Properties of $[\{Ln(NMP)_6\}(PMo_{12}O_{40})]_n$ (Ln = La, Ce, Pr; NMP = *N*-methyl-2-pyrrolidone)

Jing-Yang Niu,*[a] Mei-Lin Wei,[a] Jing-Ping Wang,*[a] and Dong-Bin Dang[b]

Keywords: Polyoxometalates / Oxo ligands / Lanthanides / Structure elucidation / Zig-zag chain

The structures of three 1:1 composite compounds prepared with the polyoxometalate (POM) $[PMo_{12}O_{40}]^{3-}$ and the cations $[Ln(NMP)_6]^{3+}$ [Ln = La (**1**), Ce (**3**), Pr (**2**); NMP = *N*-methyl-2-pyrrolidone] exhibit two types of zig-zag chains with alternating cations and anions through Mo–O_t–Ln–O_t–Mo links in the crystal. The compounds were characterized by IR, UV, and ESR spectroscopy, single-crystal X-ray structural analysis, and by a study of their thermal properties. In all the compounds, the La^{3+}, Pr^{3+}, and Ce^{3+} centers are eight-coordinate with the oxygen atoms in bicapped trigonal-prismatic geometries. The variation of the average Ln–O separations along the La, Ce, and Pr series is consistent with the effects of the lanthanide contraction. The results of the single-crystal X-ray diffraction analyses and the IR spectroscopic studies are in agreement and both show the metal cation units are coordinatively bonded to the Keggin clusters. The UV spectra of the title compounds suggest that their structures are entirely disrupted in dilute solution. Low-temperature ESR spectra indicate that thermal electron delocalization occurs among the Mo atoms in the three compounds. The results of cyclic voltammetry (CV) show that compounds **1**, **2**, and **3** all undergo five two-electron reversible reductions and that the $[PMo_{12}O_{40}]^{3-}$ anions are the active centers for electrochemical redox reactions in solution, while the corresponding cations have only a small effect on the electrochemical properties. Studies of magnetic properties show that **1** is diamagnetic, while **2**and **3** exhibit antiferromagnetic Pr–Pr or Ce–Ce exchange interactions. In addition to the results of CV, the average bond lengths and the magnetic properties of compound **3** indicate that the oxidation state of cerium is iii in the compound of formula $[\{Ce(NMP)_6\}(PMo_{12}O_{40})]_n$.

Introduction

As a rich and diverse class of inorganic cluster systems, the polyoxometalate ions formed by the early transition metals are noted for their fascinating structural, electrochemical, catalytic, magnetic, medicinal, and photophysical properties.[1] In the field of designing and assembling molecular-based materials[2−10] with structures based on the so-called anion-cation salts or host-guest solids, polyoxometalates have been found to be extremely versatile inorganic building blocks due to their ability to accept electrons.[11] So far, many intermolecular complexes based on polyoxometalates have been synthesized and reported.[11−23] Through electron transfer between organic units and polyanions, some are able to enhance the SHG (second harmonic generation) nonlinear optical response[12] while others enhance electric or magnetic properties.[13−18] The interactions existing in the structures of organic substrates and heteropoly acids or salts are mainly facilitated by hydrogen bonds, van der Waals forces, and electrostatic forces. However, infinitely extended chains based on Keggin- or Dawson-type anions and joined together by W(Mo)−O_t−M[19] links are relatively rare. Structurally characterized notable examples include $[ET]_8[PMnW_{11}O_{39}]\cdot 2H_2O$ [ET = bis(ethylenedithio)tetrathiafulvalene],[20] $[NEt_3H]_5[XCoW_{11}O_{39}]\times 3H_2O$ (X = P or As),[21] $[Cu(en)_2(OH_2)]_2[H_2en][\{Cu(en)_2\}\text{-}P_2CuW_{17}O_{61}]\times 5H_2O$ (en = ethylenediamine), $[Cu(en)_2(OH_2)]_2[Cu(en)]_{0.5}\text{-}[H_2en]_{0.5}[\{Cu(en)_2\}P_2CuW_{17}O_{61}]\times 5H_2O$,[22] $[\{Ba(DMSO)_5\text{-}(H_2O)\}_2(SiMo_{12}O_{40})]$, $[\{Ba(DMSO)_3(H_2O)_3\}\{Ba(DMSO)_5\text{-}(H_2O)GeMo_{12}O_{40}\}]$,[11] and $[\{Ca(DMF)_5\}_2SiMo_{12}O_{40}]_n$.[23]

In polyoxometalate chemistry, one of the major challenges is the "rational" synthesis of new compounds. The development of rational methods for the modification and functionalization of polyoxometalate systems may provide the means to fully exploit the desirable attributes mentioned above. From the standpoint of molecular design, we attempted to use traditional synthesis to realize such molecular assemblies. Firstly, we introduced metal ions into the framework formed by polyanions and organic units, so that

[a] School of Chemistry and Chemical Engineering, Henan University, Kaifeng 475001, P. R. China
E-mail: jyniu@henu.edu.cn.
[b] State Key Laboratory of Coordination Chemistry, Nanjing University, Nanjing 210093, P. R. China
Supporting information for this article is available on the WWW under http://www.eurjic.org or from the author.

  DOI: 10.1002/ejic.200300048

the combination of polyanions and organic units through metal ions could be achieved. Here, we chose lanthanide(III) metal ions, which have potential uses in bioinorganic chemistry and materials science.[24−26] Secondly, we chose NMP molecules as electron donors, since polyoxometalate anions are good electron acceptors, thus, they can interact leading to electron transfer. In this paper, we report the synthesis and single-crystal X-ray structural analyses of three infinitely extended polyoxometalate-based composites: $[\{Ln(NMP)_6\}(PMo_{12}O_{40})]_n$ (Ln = La, Ce, Pr; NMP = *N*-methyl-2-pyrrolidone). In the structures of these composites, the rare-earth ions are firstly coordinated by six NMP and polyanionic ligands to form a structural unit. These structural units are then connected through $Mo-O_t-Ln-O_t-Mo$[19] links to form one-dimensional chain-like structures. To the best of our knowledge, the types of structure exhibited by these compounds have not been previously reported. This paper reports studies of the magnetic and electrochemical properties as well as solid-state structural aspects of three organic-inorganic complexes with novel structures, in which infinite stacking assemblies between polyanions and cationic units have been achieved.

Results and Discussion

Experiments demonstrated that selection of a suitable solvent was crucial for growing crystals of the title compounds. Stable crystals of compounds **1**, **2**, and **3** were obtained from acetonitrile/water mixtures at room temperature. Compounds **1**, **2**, and **3** are all soluble in CH_3CN and its mixtures with water. When **1**, **2**, and **3** were dissolved in pure CH_3CN, irregular crystals were obtained because of rapid loss of solvent, therefore necessitating control of the concentration rate of the solution. This problem was overcome by simply adding water to the acetonitrile solutions. Using this method, crystals suitable for X-ray diffraction were eventually obtained. In addition, exposure of the solutions to sunlight was avoided as a result of the photosensitivity of the crystals, the reasons for which have been mentioned above.

The structures of the three composite compounds constructed from $[PMo_{12}O_{40}]^{3-}$ and the cations $[Ln(NMP)_6]^{3+}$ (Ln = La, Ce, Pr) exhibit two types of zig-zag chains with alternating cations and anions through $Mo-O_t-Ln-O_t-Mo$ links in the crystal. The novelty of these composite compounds is based on the fact that the alternating chains now contain only one cation per anion instead of two[11,23] (which is the usual case observed in other POM-cation chains). $[\{La(NMP)_6\}(PMo_{12}O_{40})]_n$ and $[\{Pr(NMP)_6\}(PMo_{12}O_{40})]_n$ show the same zig-zag chains (Figure 1). Representative molecular structural units and the coordination environment of compound **1** are shown in Figures 2 and 3(a). However, $[\{Ce(NMP)_6\}(PMo_{12}O_{40})]_n$ forms different zig-zag chains (Figure 4) from **1** and **2**, with molecular structural units and the coordination environments shown

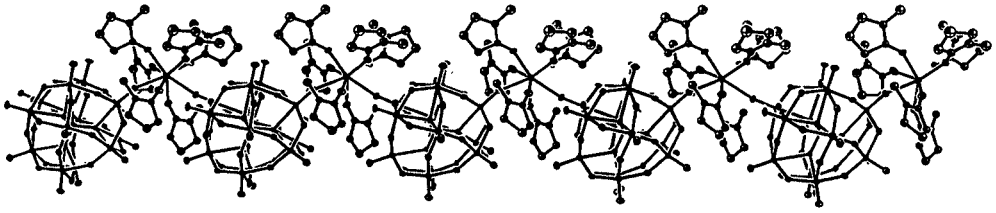

Figure 1. View of the one-dimensional chains in **1** and **2**; hydrogen atoms are omitted for clarity

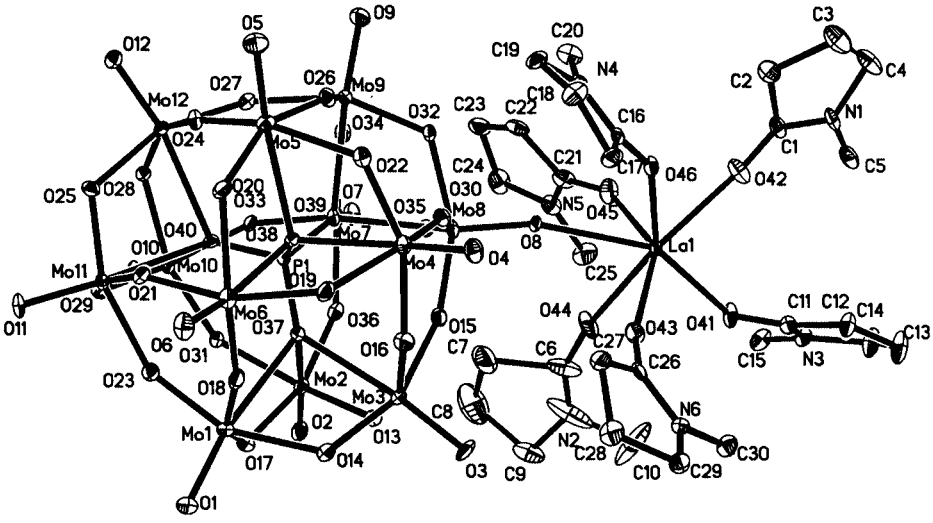

Figure 2. Molecular structural unit with atomic labeling for compound **1**; ellipsoids are shown at the 30% probability level; hydrogen atoms are omitted for clarity

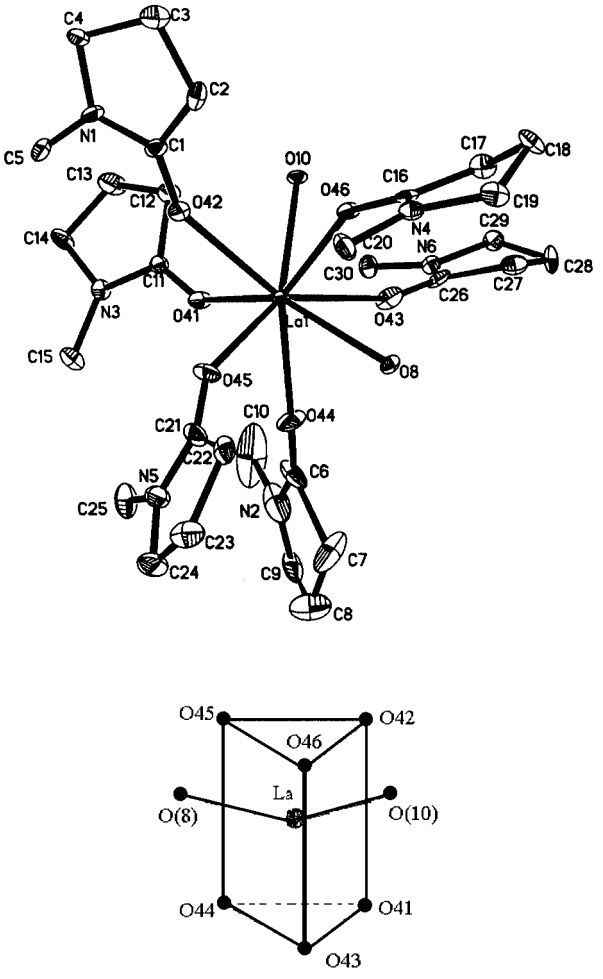

Figure 3. (a; top) Coordination environment of La^{3+} in **1**, hydrogen atoms are omitted for clarity; (b; bottom) coordination polyhedron around La^{3+} in **1**

in Figures 5 and 6. The coordination numbers of the La^{3+}, Pr^{3+} and Ce^{3+} ions are all 8 (six O atoms from the NMP ligands, and the remaining two O atoms from two adjacent heteropolyanions). The coordination environments of the La^{3+}, Pr^{3+}, and Ce^{3+} ions can be described as bicapped trigonal-prismatic, an example being that of La^{3+} shown in Figure 3(b). This is one of the common coordination geometries for complexes with a coordination number of 8.[27] In the three compounds each La^{3+}, Pr^{3+}, and Ce^{3+} ion has six O atoms from six NMP molecules forming two trigonal planes, and two terminal oxygen atoms from the polyanions occupying the caps due to the steric hindrance of the polyanions. These factors all contribute towards the stability of the title compounds. In addition, the O(10)#1−La(1)−O(8) bond angle is 124.27(15)°, the O(10)#1−Pr(1)−O(8) bond angle is 124.8 (3)°, and the O(6)#1−Ce(1)−O(6) bond angle is 122.4(3)° resulting in the formation of zig-zag chains. Comparing **3** with **1** and **2**, the striking difference lies in the type of zig-zag chains observed. In **1** and **2**, for each $[PMo_{12}O_{40}]^{3-}$ unit, there are two terminal coordinating oxygen atoms, O(10) and O(8) are almost at 90° in the Keggin-type cage while in **3**, O(6) and O(6)#1 are almost in a *para* position.

The La−O, Pr−O, and Ce−O bond lengths range from 2.397 to 2.660 Å, from 2.347 to 2.592 Å, and from 2.388 to 2.649 Å, respectively. The average bond length for all La−O bonds is 2.474 Å, which is 0.028 Å longer than the La−O1A bond length (2.446 Å) in $[La^{III}(NITBzImH)_4](ClO_4)_3\times2THF\times2H_2O$ (NITBzImH = nitronyl nitroxide radicals),[27] in which the coordination number is 8 and the coordination polyhedron around the La^{3+} ion is distorted from dodecahedral toward a square-antiprismatic geometry. This bond is 0.006 Å shorter than the La−O1A bond (2.48 Å) in $[La^{III}(NITMeBzImH)_4](ClO_4)_3\times2THF\times1H_2O$ (NITMeBzImH = nitronyl nitroxide radicals),[27] in which the coordination number of the La^{3+} ion is 8 and the coordination polyhedron around the La^{3+} ion is a distorted cube. The average bond length for all Pr−O bonds is 2.429 Å, which is 0.099 Å longer than the mean Pr(1)−O bond length (2.393 Å) of $[Pr_2(bbpen)_2(NO_3)(H_2O)]NO_3\times CH_3OH$,[28] in which the coordination number of the Pr^{3+} ion is 8 and the coordination polyhedron around the Pr^{3+} ion is a distorted cube. The average bond length for all Ce−O bonds is 2.47 Å, which is 0.064 Å shorter than the mean Ce(1)−O bond length of 2.53 Å in $[(THF)_3Ce(SC_6F_5)_3]_2$,[29] in which the coordination number of the $Ce^{3+}(1)$ ion is 8. The variation of the Ln−O average bond separations along the La, Ce, and Pr series (La−O > Ce−O > Pr−O) is consistent with the effects of the lanthanide contraction (ionic radius: $La^{3+} > Ce^{3+} > Pr^{3+}$). The fact that the mean La−O(NMOP), Pr−O(NMP), and Ce−O(NMP) bond lengths of 2.361, 2.387, and 2.405 Å, respectively, are 0.257, 0.169, and 0.244 Å shorter than the corresponding La−O_t, Pr−O_t, and Ce−O_t distances of 2.618, 2.556, and 2.649 Å indicates that the Ln−O(NMP) bonds are more stable than the Ln−O_t bonds. This is probably because the charge density at the oxygen atom of C=O is larger than that of O_t, resulting from the electron-donating effect of the methyl groups through the N atoms in the NMP molecules and the electron-withdrawing effect of the polyanions.

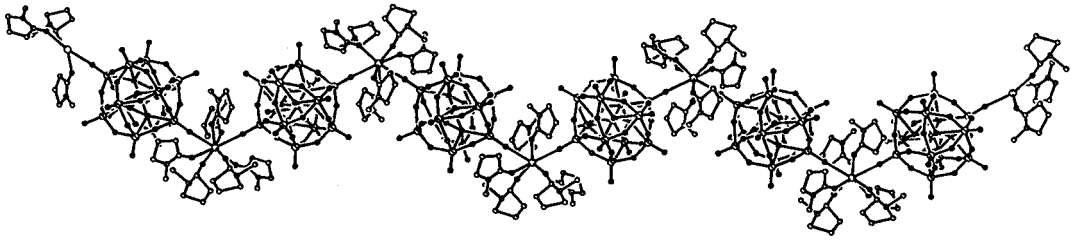

Figure 4. View of the one-dimensional chain in **3**; hydrogen atoms are omitted for clarity

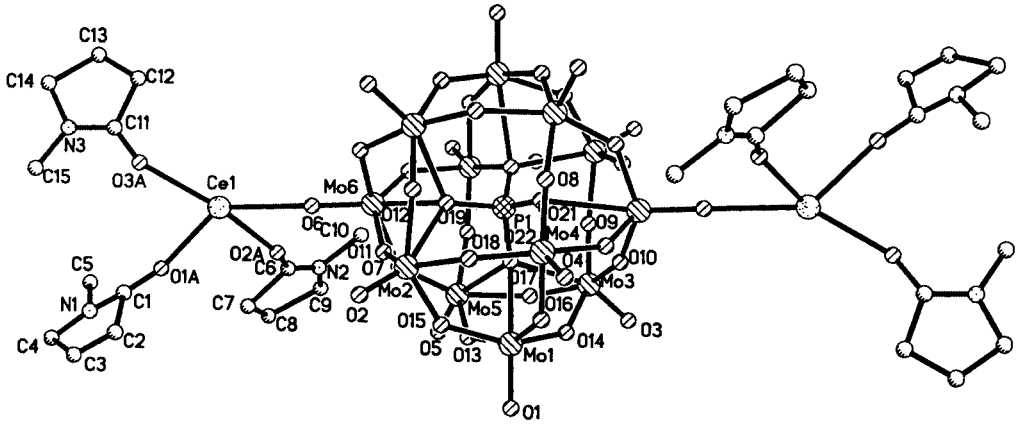

Figure 5. Molecular structural unit with atomic labeling of **3**; ellipsoids are shown at the 30% probability level; hydrogen atoms are omitted for clarity

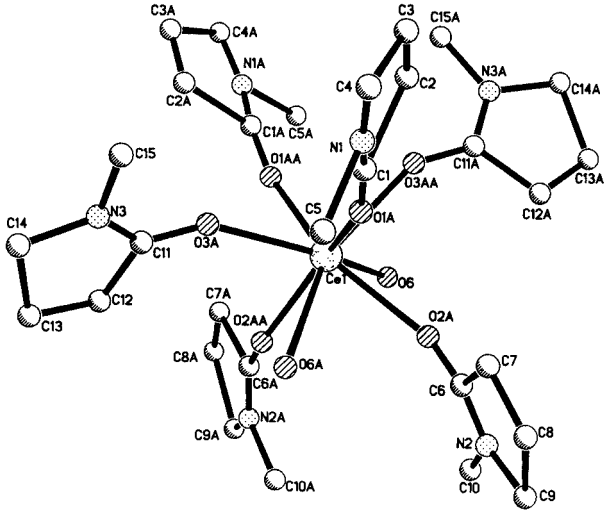

Figure 6. Coordination environment of Ce^{3+} in **3**; hydrogen atoms are omitted for clarity

The P−O bond lengths range from 1.521 to 1.546 Å for **1**, from 1.523 to 1.550 Å for **2**, and from 1.438 to 1.604 Å for **3**, respectively, with the O−P−O bond angles ranging from 108.4 to 109.9° for **1**, from 108.3 to 110.5° for **2**, and from 103.7 to 116.5° for **3**, respectively, indicating that the PO_4 tetrahedrons are distorted to a different extent in each case. The $Mo-O_t$ bond lengths range from 1.663 to 1.689 Å (av. 1.676 Å) for **1**, from 1.651 to 1.697 Å (av. 1.674 Å) for **2**, and from 1.633 to 1.664 Å (av. 1.650 Å) for **3** while the $Mo-O_a$[19] bond lengths range from 2.380 to 2.452 Å (av. 2.416 Å) for **1**, from 2.394 to 2.462 Å (av. 2.428 Å) for **2**, and from 2.384 to 2.483 Å (av. 2.427Å) for **3**. Finally, the $Mo-O_{b,c}$[19] bond lengths range from 1.804 to 2.023 Å for **1**, from 1.776 to 2.041 Å for **2**, and from 1.688 to 2.178 Å for **3**. These observations show that the MoO_6 octahedra of the polyanions in the title compounds are severely distorted because of the influence of the outer coordinating cations. Clearly, although the La^{3+}, Pr^{3+}, and Ce^{3+} ions in the title compounds have the same coordination number and coordination polyhedra, the Ce^{3+} ions distort the $[PMo_{12}O_{40}]^{3-}$ units to a larger extent than do the La^{3+} and Pr^{3+} ions. Moreover, the $Mo-O_t-Ln-O_t-Mo$ (Ln = La, Ce, Pr) links are important, firstly because polyoxometalates as ligands are electron acceptors which, in some cases, can be reduced by one or more electrons, giving rise to mixed-valence clusters. Secondly, because rare-earth atoms with magnetic properties have been introduced into the structures of compounds **1**, **2**, and **3**, they may have the potential to become novel solid-state materials in which delocalized electrons coexist with localized magnetic moments, thus affording the opportunity for the investigation of molecular systems combining magnetic and conducting properties.

There are four characteristic asymmetric vibrations resulting from heteropolyanions with the Keggin structure, namely $\nu_{as}(Mo=O_t)$, $\nu_{as}(Mo-O_b)$, $\nu_{as}(Mo-O_c)$, and $\nu_{as}(P-O_a)$. Upon comparison of the IR spectra of the title compounds with those of α-$H_3PMo_{12}O_{40}\times nH_2O$[30] the vibrational bands of the $Mo=O_t$ bonds exhibit red shifts from 975 to 961 cm^{-1} in **1**, from 975 to 959 cm^{-1} in **2** and from 975 to 961 cm^{-1} in **3**. The peaks due to the $Mo-O_c$ bonds show red shifts from 810 to 804 cm^{-1} in **1**, from 810 to 801 cm^{-1} in **2** and from 810 to 803 cm^{-1} in **3**. Lastly, the $P-O_a$ bond vibrations show red shifts from 1067 to 1063 cm^{-1} for **1**, **2**, and **3**, while the vibrational bands of the $Mo-O_b$ bonds exhibit blue shifts from 870 to 881 cm^{-1}in **1** and **3**, and from 870 to 878 cm^{-1} in **2**. These results indicate that the polyanions in the title compounds still retain the basic Keggin structure, but are distorted due to the effects of coordination. This is in agreement with the results of the single-crystal X-ray diffraction studies. In addition, there are three characteristic asymmetric vibrations resulting from NMP molecules, namely $\nu_{as}(C=O)$ (1666.1 cm^{-1}), $\nu_{as}(C-N)$ (1506 cm^{-1}), and $\nu_{as}(N-CH_3)$ (1114 cm^{-1}).[31] Upon comparison of the IR spectra of the title compounds with those of NMP molecules,[31] $\nu_{as}(C=O)$ is lower by 25.3 cm^{-1} (from 1666.1 to 1640.8 cm^{-1}) in **1**, 28.2 cm^{-1} (from 1666.1 to 1637.9 cm^{-1}) in **2**, and 27.1 cm^{-1} (from 1666.1 to 1639 cm^{-1}) in **3**, confirming that the NMP ligands are coordinated to the rare-earth ions by means of their oxygen atoms. The $\nu_{as}(C-N)$ and $\nu_{as}(N-CH_3)$ frequencies in the

three compounds rise slightly by 8 cm^{-1} and 2−6 cm^{-1}, respectively. This can be explained by the fact that the charge density at the oxygen and carbon centers is decreased due to the O atoms of the C=O bonds being coordinated to the rare-earth ions, leading to an increase in the electron-donating effect of the methyl groups through the N atoms. The IR spectroscopic studies show that there are strong interactions between the polyanions and the organic groups in the solid state.

The UV spectra of compounds **1**, **2**, and **3** measured in aqueous solution are similar to that of α-$H_3PMo_{12}O_{40}\times nH_2O$ in the same solution. There are absorption peaks at approximately 205 nm, which can be assigned to the $O_t\rightarrow Mo$ charge-transfer bands which are also strong due to the absorption of NMP molecules at the same wavelength.[31] This suggests that although the compounds exist in polymeric form in the solid state, the polymeric chains are entirely disrupted in dilute solution. This has been observed in a previous study.[12]

The three complexes are strongly photosensitive towards irradiation with sunlight, resulting in charge-transfer by oxidation of the NMP moieties and reduction of the $[PMo_{12}O_{40}]^{3-}$ groups. ESR spectra of powders of the title compounds after exposure to sunshine are typical of molybdenum(v).[32−33] At 110 K, $g = 1.949$ for **1**, $g = 1.947$ for **2**, and $g = 1.948$ for **3**. Observation of an intense, relatively narrow ESR signal from about 3460 to 3500 G (40 G peak to peak) for **1**, **2**, and **3** at 110 K indicates that intramolecular electron transfer is relatively slow on the ESR timescale, and that the electron is delocalized.

Table 1. Cathodic peak potentials (E_{cp}) and anodic (E_{ap}) and potential differences for α-$H_3PMo_{12}O_{40}\times nH_2O$ and compounds **1** and **2** (in a mixture of 50% 1,4-dioxane and 50% H_2O containing 0.5 mol/L H_2SO_4 as the supporting electrolyte, sensitivity 10 μA, $v = 50$ mV·s^{-1}, SCE as the reference electrode)

Compound	E_{cp} [V]	E_{ap} [V]	ΔE_p [mV]	$E_{1/2}$ [V]
α-$H_3PMo_{12}O_{40}\times nH_2O$	0.308	0.339	31	0.324
	0.179	0.208	29	0.194
	−0.052	−0.022	30	−0.037
	−0.201	−0.17	31	−0.186
	−0.282	−0.244	38	−0.263
1	0.311	0.341	30	0.326
	0.181	0.212	31	0.197
	−0.050	−0.019	31	−0.035
	−0.208	−0.176	32	−0.192
	−0.286	−0.247	39	−0.267
2	0.308	0.340	32	0.324
	0.181	0.212	31	0.197
	−0.053	−0.022	31	−0.038
	−0.208	−0.179	29	−0.194
	−0.288	−0.249	39	−0.269
3	0.304	0.338	34	0.321
	0.177	0.209	32	0.193
	−0.058	−0.021	37	−0.040
	−0.210	−0.174	36	−0.192
	−0.303	−0.262	41	−0.283

Table 1 summarizes the cathodic and anionic peak potentials [V], the half-wave potentials $E_{1/2}$ [V], as well as the difference potentials for α-$H_3PMo_{12}O_{40}\times nH_2O$ and compounds **1**, **2**, and **3** (in a mixture of 50% 1,4-dioxane and 50% H_2O containing 0.5 mol/L H_2SO_4 as the supporting electrolyte, sensitivity 10 μA, $v = 50$ mV·s^{-1}, SCE as the reference electrode). Figure 7 shows the CVs for α-$H_3PMo_{12}O_{40}\times nH_2O$ and compounds **1**, **2**, and **3** carried out at a sensitivity of 10 μA. For phospho-polyoxomolybdate it is difficult to obtain well-defined redox waves in cyclic voltammetry in aqueous electrolytes due to the ease of hydrolysis of $[PMo_{12}O_{40}]^{3-}$. However, it can be stabilized by addition of comparatively large amounts of organic solvents. Thus, cyclic voltammetry was measured in organic/aqueous solvent mixtures (50% 1,4-dioxane and 50% redistilled H_2O) containing 0.5 mol/L H_2SO_4 as the supporting electrolyte. α-$H_3PMo_{12}O_{40}\times nH_2O$ as well as compounds **1**, **2**, and **3** all undergo five two-electron reversible reductions. The reversibility criterion used was $\Delta E_p = E_{ap} - E_{cp} = 59/n$ mV (n = number of electrons). The small difference in $E_{1/2}$ [V] of the three compounds shows that the $[PMo_{12}O_{40}]^{3-}$ anions are the active centers for electrochemical redox activity in the solutions, while the corresponding cations have only a small effect on the electrochemical redox behavior. Upon comparison of the results of the CVs of the three compounds, it was found that the effect of $[Ce(NMP)_6]^{3+}$ on the electrochemical redox behavior of $[PMo_{12}O_{40}]^{3-}$ is stronger than that of $[La(NMP)_6]^{3+}$ or $[Pr(NMP)_6]^{3+}$.

In aqueous solution, cerium has two accessible oxidation states namely III and IV. Only strong oxidants such as permanganate and peroxodisulfate can oxidize Ce^{III}. In general, the determination of the oxidation state of cerium is frequently a difficult problem. Previous work has shown that selected heteropolyoxotungstates can significantly influence the behavior of complex f-ions. In 1971, Peacock and Weakley reported that heteropolyoxotungstates could stabilize tetravalent cerium.[34] This stabilization was apparent from the ease of oxidation of Ce^{IV} in $[Ce(PW_{11}O_{39})_2]$, $[Ce(SiW_{11}O_{39})_2]$ and $[Ce(P_2W_{17}O_{61})_2]$. In aqueous solution, these oxidations were found to occur at +0.6 to +0.9 V vs. Ag/AgCl, which is less than the standard reduction potential of Ce^{IV}. More recently, Haraguchi et al.[35] have confirmed the shifts of the Ce^{III}/Ce^{IV} redox potentials in these heteropolyoxotungstates. The implication of their work is that the oxidation of Ce^{III} is possible with the use of only mild oxidants.[36] In contrast, the shifts of the Ce^{III}/Ce^{IV} redox potentials in heteropolymolybdates have not been reported and consequently we have examined the shift of the Ce^{III}/Ce^{IV} redox potential in $[\{Ce(NMP)_6\}(PMo_{12}O_{40})]_n$.

Figure 8 (A and B) shows the CVs of α-$H_3PMo_{12}O_{40}\times nH_2O$ (1 mmol/L) and compound **3** (1 mmol/L) in a mixture of 50% 1,4-dioxane and 50% H_2O containing 0.5 mol/L H_2SO_4 as the supporting electrolyte with Ag/AgCl as the reference electrode. Figure 8 (C) depicts the CV of compound **3** (1 mmol/L) in a mixture of 50% 1,4-dioxane and 50% H_2O containing 1.0 mol/L $HClO_4$ as the supporting electrolyte with Ag/AgCl as the reference electrode. In contrast, it was found that Ce^{III} in $[\{Ce(NMP)_6\}(PMo_{12}O_{40})]_n$ cannot be oxidized to Ce^{IV} even

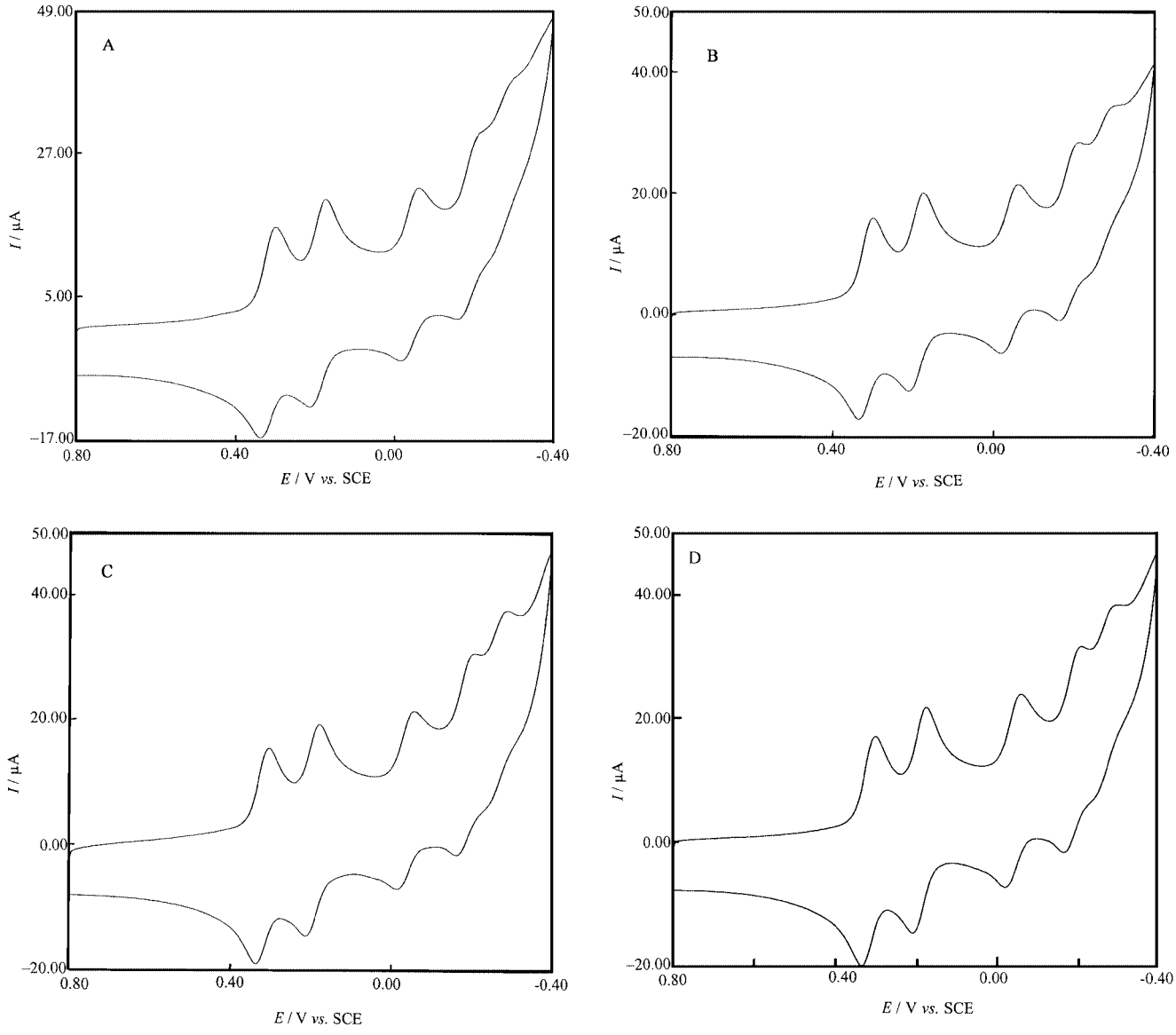

Figure 7. (A) CV of α-$H_3PMo_{12}O_{40}\times nH_2O$(1 mmol/L) in a mixture of 50% 1,4-dioxane and 50% H_2O containing 0.5 mol/L H_2SO_4 as the supporting electrolyte, sensitivity 10 μA, v = 50 mV·s^{-1}, SCE as the reference electrode; (B) CV of compound **1** (1 mmol/L) in a mixture of 50% 1,4-dioxane and 50% H_2O containing 0.5 mol/L H_2SO_4 as the supporting electrolyte, sensitivity 10 μA, v = 50 mV·s^{-1}, SCE as the reference electrode; (C) CV of compound **2** (1 mmol/L) in a mixture of 50% 1,4-dioxane and 50% H_2O containing 0.5 mol/L H_2SO_4 as the supporting electrolyte, sensitivity 10 μA, v = 50 mV s^{-1}, SCE as the reference electrode; (D) CV of compound **3** (1 mmol/L) in a mixture of 50% 1,4-dioxane and 50% H_2O containing 0.5 mol/L H_2SO_4 as the supporting electrolyte, sensitivity 10 μA, v = 50 mV s^{-1}, SCE as the reference electrode

under rigorous conditions (+1.5 V vs. Ag/AgCl; electrolyte 1 mol/L $HClO_4$ purged with O_2). These conditions are sufficient to oxidize the noncomplexed Ce^{III} aqua ion. The Ce^{III} ion in compound **3** is not oxidized at potentials higher than would be required for its oxidation in noncomplexing media, indicating a stabilization of Ce^{III} in this case. In addition, the solution chemistry of cerium(III) is similar to that of Zr, Hf and, particularly, tetravalent actinides. Thus, Ce^{III} gives phosphates insoluble in 4 mol/L HNO_3 and iodates insoluble in 6 mol/L HNO_3, as well as an insoluble oxalate. Upon addition of 5 mL of 4 mol/L NaOH to 20 mL of an aqueous solution of 1 mmol of $[\{Ce(NMP)_6\}(PMo_{12}O_{40})]_n$, which dissociates into small molecules, white deposited material can be observed. Filtration of the mixture to recover the solid, which is soluble in 5 mL of dilute HCl (0.5 mol/L), followed by the addition of two drops of concentrated phosphoric acid to the resultant solution produces a white precipitate which is soluble in 4 mol/L HNO_3.

Finally, the average $Ce^{III}-O$ distance in compound **3** is 2.47 Å, which is essentially the same as the sum of the Ce and O ionic radii of 2.49 Å for eight-coordinate Ce and two-coordinate O centers.[36]

Thus, based on the results of CV, the solution chemistry, the average bond lengths and the following magnetic susceptibilities, we can conclude that $[\{Ce(NMP)_6\}(PMo_{12}O_{40})]_n$ contains a tervalent cerium center.

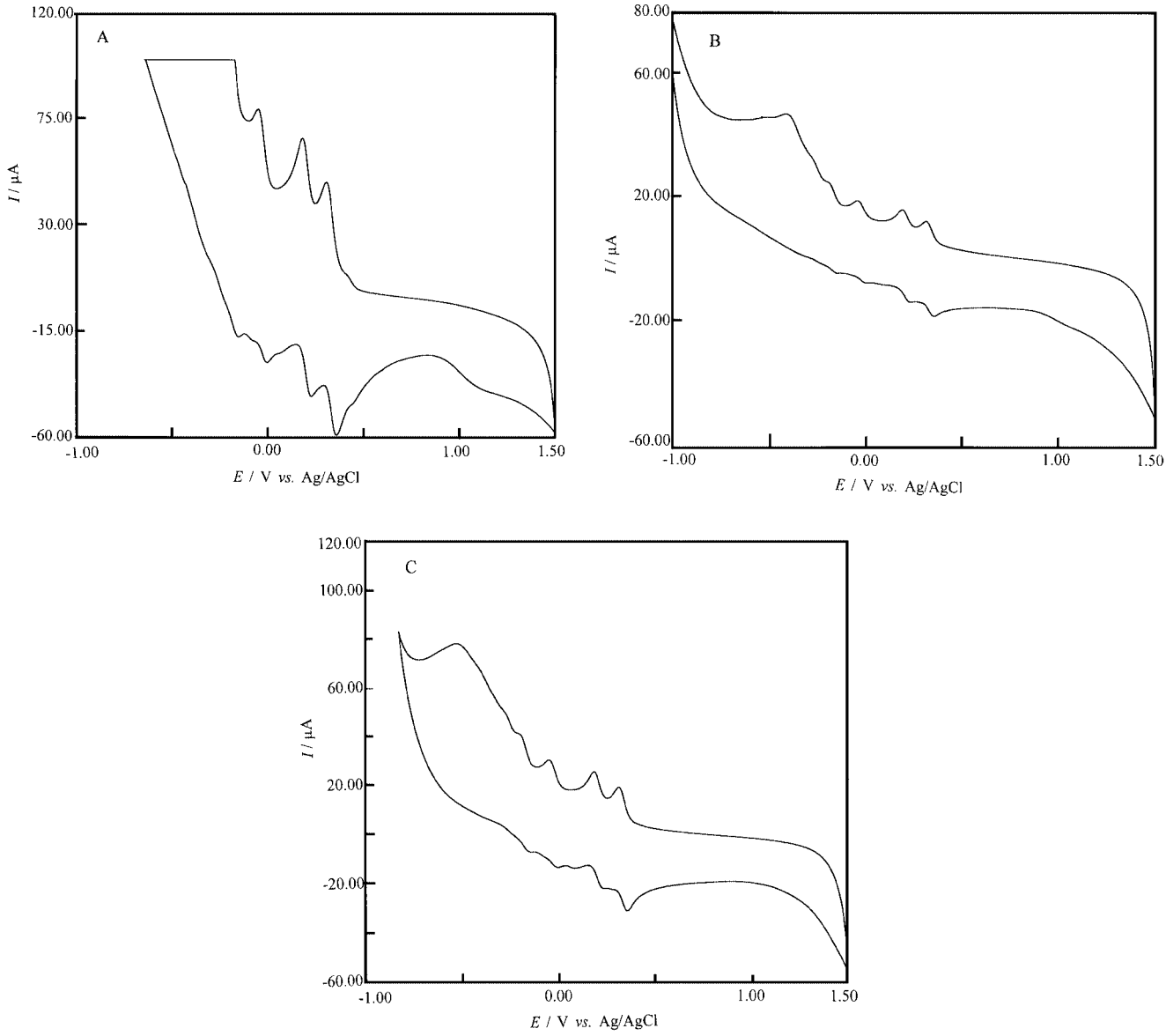

Figure 8. (A) CV of α-$H_3PMo_{12}O_{40}\times nH_2O$ (1 mmol/L) in a mixture of 50% 1,4-dioxane and 50% H_2O containing 0.5 mol/L H_2SO_4 as the supporting electrolyte, sensitivity 10 μA, v = 50 mV·s^{-1}, Ag/AgCl as the reference electrode; (B) CV of compound **3** (1 mmol/L) in a mixture of 50% 1,4-dioxane and 50% H_2O containing 0.5 mol/L H_2SO_4 as the supporting electrolyte, sensitivity 10 μA, v = 50 mV·s^{-1}, Ag/AgCl as the reference electrode; (C) CV of compound **3** (1 mmol/L) in a mixture of 50% 1,4-dioxane and 50% H_2O containing 1.0 mol/L $HClO_4$ as the supporting electrolyte, sensitivity 10 μA, v = 50 mV s^{-1}, Ag/AgCl as the reference electrode

The variable-temperature magnetic susceptibilities of polycrystalline powders of the three compounds were measured with a Cahn-2000 magnetometer between 75 and 300 K. The studies of magnetic properties show that compound **1** is diamagnetic, while compounds **2**and **3** exhibit antiferromagnetic Pr−Pr or Ce−Ce exchange interactions. The results are displayed in the form of $1/\chi_M$ (the molar magnetic susceptibility per formula unit) vs. absolute temperature in Figures 9 and 10 for compounds **2** and **3**. The mean molar magnetic susceptibility of $[\{La(NMP)_6\}(PMo_{12}O_{40})]_n$ (**1**) (−0.00018 cm^3·mol^{-1}) was used as a diamagnetic correction for the molar magnetic susceptibilities of **2** and **3**. The magnetic data for compounds **2** and **3** have been fitted to the Curie−Weiss law $\chi_M = C/(T - \theta)$ and $\chi_M = Ng^2\beta s\ (s + 1)/3k(T - \theta)$ (s_{Ce} = 1/2; s_{Pr} = 1). The Weiss constants $\theta_{Pr} = -58.88$ and $\theta_{Ce} = -108.78$ show that there are strong antiferromagnetic Pr−Pr or Ce−Ce exchange interactions in **2** and **3**.

Conclusions

Three one-dimensional composite compounds have been prepared based on the polyoxometalate anion $[PMo_{12}O_{40}]^{3-}$ and the cations $[LnNMP]_6]^{3+}$ (Ln = La, Ce, Pr). Single-crystal X-ray diffraction studies showed that the three compounds exhibit two types of zig-zag chains with alternating cations and anions through Mo−O_t−Ln−

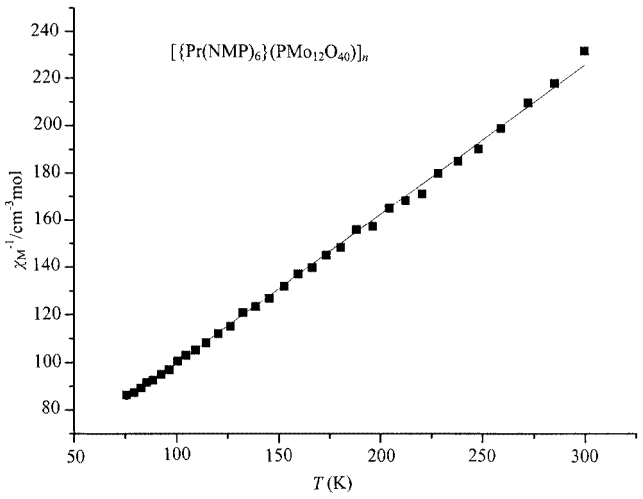

Figure 9. Plot of inverse molar susceptibility vs. absolute temperature for compound **2** (black squares); the solid line represents the best fit of the data with value in the text

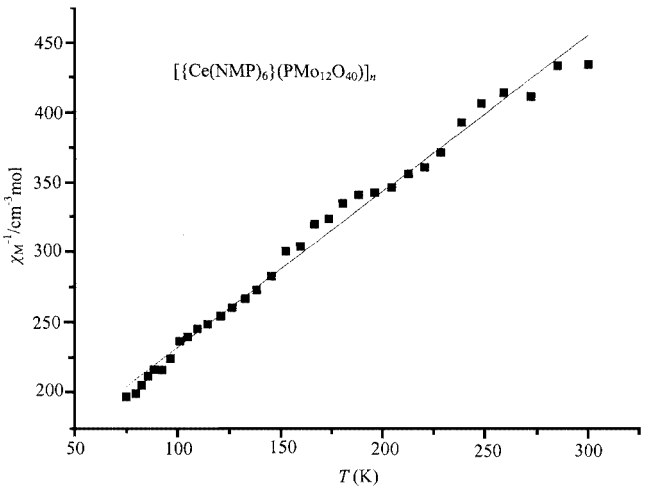

Figure 10. Plot of molar susceptibility vs. absolute temperature for compound **3** (black squares); the solid line represents the best fit of the data with value in the text

O_t−Mo links in the crystal. The variation of the Ln−O average bond separations along the La, Ce, and Pr series is consistent with the effects of the lanthanide contraction (ionic radius: $La^{3+} > Ce^{3+} > Pr^{3+}$) and the polyanions in the title compounds are severely distorted as a result of the influence of the outer coordinating cations. The polymeric structures of the compounds are entirely disrupted in dilute solution, and the cyclic voltammograms measured show that the three compounds all undergo five two-electron reversible reductions. The studies of magnetic properties indicate that **1** is diamagnetic while **2** and **3** exhibit antiferromagnetic Pr−Pr or Ce−Ce exchange interactions.

Experimental Section

Materials: All organic solvents and materials used for synthesis were of reagent grade and used without further purification. α-$H_3PMo_{12}O_{40}\times nH_2O$ was prepared according to a literature method.[30] The metal chlorides $LnCl_3$ (Ln = La, Ce, Pr) were prepared by addition of concentrated HCl to Ln_2O_3 (99.9%).

Syntheses

$[\{La(NMP)_6\}(PMo_{12}O_{40})]_n$ (1), $[\{Pr(NMP)_6\}(PMo_{12}O_{40})]_n$ (2), and $[\{Ce(NMP)_6\}(PMo_{12}O_{40})]_n$ (3): The formation of heteropolyacid lanthanide salts was accomplished by neutralization of the acids. α-$H_3PMo_{12}O_{40} \times nH_2O$ (3.8 g, 2 mmol) and $LnCl_3$ (2 mmol) were dissolved in water (15 mL) and the solution was heated to dryness at 80 °C in a water bath. NMP (2 mL) was then added to the resultant dry solid (2 g) with stirring until the mixture became a paste. After standing for ca. 15 min, the paste was dissolved in a minimum of an acetonitrile/water mixture (3:2, v/v). Finally, the solution was filtered and left standing to concentrated at room temperature. After 1−2 d, yellow crystals suitable for X-ray diffraction were obtained; yield based on α-$H_3PMo_{12}O_{40} \times nH_2O$ ca. 80%. $C_{30}H_{54}LaMo_{12}N_6O_{46}P$ (**1**) (2555.95): calcd. C 14.08, H 2.11, N 3.29; found C 13.97, H 2.01, N 3.39. $C_{30}H_{54}Mo_{12}N_6O_{46}PPr$ (**2**) (2557.95): calcd. C 14.07, H 2.11, N 3.28; found C 14.07, H 2.06, N 3.39. $C_{30}H_{54}CeMo_{12}N_6O_{46}P$ (**3**) (2557.16): calcd. C 4.08, H 2.11, N 3.28; found C 14.15, H 2.13, N 3.35. TG/DTA data: **1:** Weight loss of 23.5% below 506.3 °C without an obvious endothermic peak and with two exothermic peaks at 285 °C (where the La−O bonds

Table 2. Crystal data for **1**, **2**, and **3**

	1	**2**	**3**
Empirical formula	$C_{30}H_{54}Mo_{12}N_6O_{46}PLa$	$C_{30}H_{54}Mo_{12}N_6O_{46}PPr$	$C_{30}H_{54}Mo_{12}N_6O_{46}PCe$
Formula mass	2555.95	2557.95	2557.16
Crystal size [mm]	0.39×0.33×0.29	0.61×0.48×0.46	0.30×0.26×0.18
Crystal system	monoclinic	monoclinic	monoclinic
Space group	*Pn*	*Pn*	*C*2/*c*
Z	2	2	4
a [Å]	12.954(3)	12.947(3)	25.524(5)
b [Å]	13.417(3)	13.294(3)	12.678(3)
c [Å]	18.810(4)	18.977(4)	22.723(5)
β [°]	99.67(3)	100.77(3)	112.10(3)
V [$Å^3$]	3222.6(11)	3208.7(11)	6813(2)
μ [mm^{-1}]	3.029	3.135	3.407
Total no.of reflections	10938	10472	10788
Independent reflections; R_{int}	10929; 0.0145	10472; 0.0000	5877; 0.0164
*R*1, *wR*2 [$I > 2\sigma(I)$]	0.0278, 0.0686	0.0591, 0.1531	0.0488, 0.1365

Table 3. Selected bond lengths [Å] and angles [°] for **1**

Mo(1)−O(14)	2.016(5)	Mo(4)−O(16)	1.989(5)
Mo(1)−O(37)	2.461(5)	Mo(4)−O(19)	1.994(5)
Mo(2)−O(2)	1.669(5)	Mo(4)−O(38)	2.434(4)
Mo(21)−O(36)	1.820(5)	Mo(5)−O(5)	1.682(5)
Mo(2)−O(13)	1.846(5)	Mo(5)−O(24)	1.821(5)
Mo(2)−O(17)	2.001(5)	Mo(5)−O(20)	1.841(5)
Mo(2)−O(31)	2.006(5)	Mo(5)−O(38)	2.438(5)
Mo(2)−O(37)	2.425(5)	Mo(6)−O(6)	1.678(5)
Mo(3)−O(3)	1.663(5)	Mo(6)−O(18)	1.816(5)
Mo(3)−O(16)	1.820(5)	Mo(6)−O(19)	1.846(5)
Mo(3)−O(14)	1.840(5)	Mo(6)−O(20)	1.997(5)
Mo(3)−O(13)	2.005(5)	Mo(6)−O(21)	2.018(5)
Mo(3)−O(15)	2.013(5)	Mo(6)−O(38)	2.452(5)
Mo(3)−O(37)	2.420(4)	Mo(8)−O(8)	1.687(4)
Mo(4)−O(4)	1.665(5)	Mo(10)−O(10)	1.689(5)
Mo(4)−O(30)	1.826(5)	O(10)−La(1)#2[a]	2.576(5)
O(41)−La(1)−O(10)#1[a]	73.27(16)	O(45)−La(1)−O(10)#1	148.16(18)
O(45)−La(1)−O(8)	77.15(18)	O(46)−La(1)−O(10)#1	72.47(16)
O(41)−La(1)−O(8)	150.11(16)	O(44)−La(1)−O(10)#1	129.8(2)
O(10)#1−La(1)−O(8)	124.27(15)	O(43)−La(1)−O(10)#1	68.62(17)

[a] Symmetry transformation used to generate equivalent atoms: #1: x, $y + 1$, z; #2: x, $y - 1$, z.

break with the oxidation of NMP molecules) and 474 °C (where the heteropolyanionic cages decompose to the lower oxides of the metals like MoO_3); calcd. 23.27% for six NMP units. **2:** Weight loss of 22.8% below 525 °C without an obvious endothermic peak and with two exothermic peaks at 287 °C (where the Pr−O bonds break with the oxidation of NMP molecules) and 493 °C (where the heteropolyanionic cages decompose to the lower oxides of the metals like MoO_3); calcd. 23.27% for six NMP units. **3:** Weight loss of 23.6% below 530 °C without an obvious endothermic peak and with two exothermic peaks at 282 °C (where the Ce−O bonds break with the oxidation of NMP molecules) and 465 °C (where the heteropoly anionic cages decompose to the lower oxides of the metals like MoO_3); calcd. 23.26% for six NMP units.

Methods: C, H, and N elemental analyses were performed with a Perkin−Elmer 240C elemental analyzer. IR spectra of samples were recorded in KBr pellets with a Nicolet 170 SXFT-IR spectrometer in the range of 4000−500cm^{-1}. UV spectra were recorded

Table 4. Selected bond lengths [Å] and angles [°] for **2**

Pr(1)−O(3A)	2.401(12)	Mo(4)−O(16)	1.998(9)
Pr(1)−O(1A)	2.404(9)	Mo(4)−O(38)	2.416(9)
Pr(1)−O(4A)	2.409(10)	Mo(5)−O(5)	1.670(9)
Pr(1)−O(2A)	2.416(10)	Mo(5)−O(24)	1.810(9)
Pr(1)−O(10)#1[a]	2.519(10)	Mo(5)−O(20)	1.844(10)
Pr(1)−O(8)	2.592(11)	Mo(5)−O(26)	1.999(9)
Mo(1)−O(1)	1.667(10)	Mo(5)−O(22)	1.999(10)
Mo(1)−O(23)	1.802(10)	Mo(5)−O(38)	2.423(8)
Mo(1)−O(17)	1.834(9)	Mo(6)−O(6)	1.658(11)
Mo(1)−O(18)	2.012(11)	Mo(6)−O(18)	1.802(10)
Mo(1)−O(14)	2.023(10)	Mo(6)−O(19)	1.857(9)
Mo(1)−O(37)	2.441(9)	Mo(6)−O(21)	1.990(10)
Mo(2)−O(2)	1.651(10)	Mo(6)−O(20)	2.000(11)
Mo(2)−O(36)	1.814(10)	Mo(6)−O(38)	2.462(9)
Mo(2)−O(13)	1.853(11)	Mo(8)−O(8)	1.697(11)
Mo(2)−O(31)	1.989(9)	Mo(10)−O(10)	1.695(10)
Mo(2)−O(17)	2.006(9)	O(10)−Pr(1)#2[a]	2.519(10)
Mo(2)−O(37)	2.409(9)	O(5A)−Pr(1)−O(10)#1	145.3(4)
Mo(3)−O(3)	1.666(11)	O(6A)−Pr(1)−O(10)#1	72.0(3)
Mo(3)−O(14)	1.819(10)	O(3A)−Pr(1)−O(10)#1	69.2(3)
Mo(3)−O(16)	1.822(10)	O(1A)−Pr(1)−O(10)#1	74.7(3)
Mo(3)−O(13)	1.997(11)	O(4A)−Pr(1)−O(10)#1	136.9(4)
Mo(3)−O(15)	2.041(10)	O(2A)−Pr(1)−O(10)#1	71.4(4)
Mo(3)−O(37)	2.432(9)	O(5A)−Pr(1)−O(8)	76.9(4)
Mo(4)−O(4)	1.696(11)	O(6A)−Pr(1)−O(8)	66.8(3)
Mo(4)−O(30)	1.829(10)	O(3A)−Pr(1)−O(8)	75.8(4)
Mo(4)−O(22)	1.830(9)	O(1A)−Pr(1)−O(8)	148.1(3)
Mo(4)−O(19)	1.986(9)	O(4A)−Pr(1)−O(8)	71.0(3)
O(10)#1−Pr(1)−O(8)	124.8(3)	O(2A)−Pr(1)−O(8)	130.8(4)

[a] Symmetry transformation used to generate equivalent atoms: #1: x, $y + 1$, z; #2: x, $y - 1$, z.

Table 5. Selected bond lengths [Å] and angles [°] for **3**

Ce(1)−O(1A)	2.388(7)	Mo(5)−O(7)	1.824(7)
Ce(1)−O(1A)#1[a]	2.388(7)	Mo(5)−O(17)	1.985(7)
Ce(1)−O(2A)#1	2.409(7)	Mo(5)−O(8)#2[a]	1.995(9)
Ce(1)−O(2A)	2.409(7)	Mo(5)−O(21)#2	2.483(11)
Ce(1)−O(3A)	2.418(6)	Mo(5)−O(22)	2.516(10)
Ce(1)−O(3A)#1	2.418(6)	Mo(6)−O(9)#2	1.657(12)
Ce(1)−O(6)	2.649(6)	Mo(6)−O(6)	1.664(6)
Ce(1)−O(6)#1	2.649(6)	Mo(6)−O(10)#2	1.705(12)
Mo(1)−O(1)	1.633(8)	Mo(6)−O(11)	1.866(13)
Mo(1)−O(16)	1.809(7)	O(1A)−Ce(1)−O(1A)#1	119.4(4)
Mo(1)−O(14)	1.830(7)	O(1A)−Ce(1)−O(2A)#1	144.8(3)
Mo(1)−O(15)	1.990(7)	O(1A)#1−Ce(1)−O(2A)#1	83.3(3)
Mo(1)−O(13)	2.000(7)	O(1A)−Ce(1)−O(2A)	83.3(3)
Mo(1)−O(22)	2.408(11)	O(1A)#1−Ce(1)−O(2A)	144.8(3)
Mo(1)−O(20)	2.464(11)	O(2A)#1−Ce(1)−O(2A)	92.1(4)
Mo(2)−O(2)	1.662(7)	O(1A)−Ce(1)−O(3A)	76.0(3)
Mo(2)−O(15)	1.807(8)	O(1A)#1−Ce(1)−O(3A)	74.8(3)
Mo(2)−O(11)	1.818(12)	O(2A)#1−Ce(1)−O(3A)	85.9(3)
Mo(2)−O(11′)	1.888(13)	O(2A)−Ce(1)−O(3A)	139.9(3)
Mo(2)−O(12)	1.967(13)	O(1A)−Ce(1)−O(3A)#1	74.8(3)
Mo(2)−O(18)	1.990(6)	O(1A)#1−Ce(1)−O(3A)#1	76.0(3)
Mo(2)−O(12′)	2.113(13)	O(2A)#1−Ce(1)−O(3A)#1	139.9(3)
Mo(2)−O(19)	2.396(10)	O(2A)−Ce(1)−O(3A)#1	85.9(3)
Mo(3)−O(3)	1.642(7)	O(3A)−Ce(1)−O(3A)#1	120.1(4)
Mo(3)−O(12)#2	1.688(13)	O(1A)−Ce(1)−O(6)	137.1(3)
Mo(3)−O(17)	1.807(7)	O(1A)#1−Ce(1)−O(6)	75.7(2)
Mo(3)−O(14)	1.975(9)	O(2A)#1−Ce(1)−O(6)	71.1(2)
Mo(3)−O(10)	2.034(13)	O(2A)−Ce(1)−O(6)	69.8(2)
Mo(3)−O(10′)	2.066(12)	O(3A)−Ce(1)−O(6)	144.3(3)
Mo(3)−O(19)#2	2.428(10)	O(3A)#1−Ce(1)−O(6)	70.7(2)
Mo(4)−O(4)	1.639(7)	O(1A)−Ce(1)−O(6)#1	75.7(2)
Mo(4)−O(8)	1.803(9)	O(1A)#1−Ce(1)−O(6)#1	137.1(3)
Mo(4)−O(18)	1.808(7)	O(2A)#1−Ce(1)−O(6)#1	69.8(2)
Mo(4)−O(16)	2.001(8)	O(2A)−Ce(1)−O(6)#1	71.1(2)
Mo(4)−O(9)	2.041(12)	O(3A)−Ce(1)−O(6)#1	70.7(2)
Mo(4)−O(21)	2.384(11)	O(3A)#1−Ce(1)−O(6)#1	144.3(3)
Mo(5)−O(5)	1.657(7)	O(6)−Ce(1)−O(6)#1	122.4(3)
Mo(5)−O(13)	1.795(9)	Mo(6)−O(6)−Ce(1)	176.3(4)

[a] Symmetry transformation used to generate equivalent atoms: #1: $-x$, y, $-z + 1/2$; #2: $-x - 1/2$, $-y - 1/2$, $-z$.

in aqueous solution with a UV-250 spectrometer in the range of 190−400 nm. Thermogravimetric analyses (TG/DTA) were performed in air with a Perkin−Elmer-7 instrument with a heating rate of 10 °C/min from room temperature to 600 °C. ESR spectra of powdered samples of the title compounds after exposure to sunshine were recorded with a Bruker ER-200-D-SRC spectrometer in the X-band frequency at 110 K. Cyclic voltammograms were obtained with an LK98BII electrochemical analyzer at 25 °C. A glass-carbon (diameter = 3 mm) electrode was employed as the working electrode. The electrode was subjected to ultrasonic washing for 5 min followed by washing with water and acetone prior to every measurement. A platinum rod (diameter = 2 mm) was used as the counter electrode. The reference electrode was an SCE or an Ag/AgCl electrode. A Cahn-2000 magnetometer was used to measure the temperature dependence of the magnetic susceptibilities of three compounds in the 75−300 K temperature range. The crystal structures of **1**, **2**, and **3** were determined from single-crystal X-ray diffraction data. Intensity data were collected with a Rigaku RAXIS-IV image plate area detector with Mo-K_α (λ = 0.71073 Å) radiation at 293(2) K. The structures were solved by direct methods and refined using full-matrix least-squares calculations with anisotropic displacement parameters for all non-hydrogen atoms. All hydrogen atoms were geometrically fixed to allow riding on the parent atoms to which they are attached and refined with individual isotropic displacement parameters. All calculations were performed using the SHELXTL-97 program.[37] A summary of the X-ray crystal data for the three compounds is shown in Table 2. Selected bond lengths and bond angles are listed in Tables 3, 4, and 5. CCDC-201822 (**1**), -201823 (**2**), and -201821 (**3**) contain the supplementary crystallographic data for this paper. These data can be obtained free of charge at www.ccdc.cam.ac.uk/conts/retrieving.html [or from the Cambridge Crystallographic Data Centre, 12 Union Road, Cambridge CB2 1EZ, UK; Fax: (internat.) + 44-1223/336-033; E-mail: deposit@ccdc.cam.ac.uk].

Acknowledgments

This work was supported by the Natural Science Foundation of Henan Province and the Outstanding Youth Foundation of Henan Province.

[1] [1a] M. T. Pope, *Heteropoly- and Isopoly-Oxometalates*, Springer-Verlag, New York, **1983**. [1b] M. T. Pope, A. Müller, *Angew. Chem. Int. Ed. Engl.* **1991**, *30*, 34. [1c] *Polyoxometalates: From Platonic Solids to Anti-Retroviral Activity* (Eds.: M. T. Pope, A. Müller), Kluwer Academic Publishers, Dordrecht, The Netherlands, **1994**. [1d] *Chem. Rev.* **1998**, *98*, 8 (Guest Ed.: C. L. Hill).

[2] E. Coronado, C. Gomez-Garcia, *Chem. Rev.* **1998**, *98*, 273.
[3] [3a] M. I. Khan, E. Yohannes, D. Powell, *Inorg. Chem.* **1999**, *38*, 212−213. [3b] M. I. Khan, E. Yohannes, D. Powell, *Chem. Commun.* **1999**, 23−24.
[4] M. I. Khan, *J. Solid State Chem.* **2000**, *152*, 105−112.
[5] M. Sadakane, M. H. Dickman, M. T. Pope, *Angew. Chem. Int. Ed.* **2000**, *39*, 2914−2916.
[6] H. Choi, Y.-U. Kwon, O. H. Han, *Chem. Mater.* **1999**, *11*, 1641−1643.
[7] L. G. Beauvais, M. P. Shores, J. R. Long, *Chem. Mater.* **1998**, *10*, 3783−3786.
[8] M. P. Shores, L. G. Beauvais, J. R. Long, *Inorg. Chem.* **1999**, *38*, 1648−1649.
[9] M. P. Shores, L. G. Beauvais, J. R. Long, *J. Am. Chem. Soc.* **1999**, *121*, 775−779.
[10] J.-H. Son, H. Choi, Y.-U. Kwon, *J. Am. Chem. Soc.* **2000**, *122*, 7432−7433.
[11] J.-Y. Niu, Q. Wu, J.-P. Wang, *J. Chem. Soc., Dalton Trans.* **2002**, 2512−2516.
[12] [12a] J.-Y. Niu, X.-Z. You, C.-Y. Duan, H.-K. Fun, Z.-Y. Zhou, *Inorg. Chem.* **1996**, *35*, 4211−4216. [12b] J.-Y. Niu, J.-P. Wang, W. Chen, C.-H.-L. Kennard, K.-A. Byriel, *J. Coord. Chem.* **2001**, *53*, 153−162. [12c] J.-Y. Niu, X.-Z. You, H.-K. Fun, Z.-Y. Zhou, B.-C. Yip, *Polyhedron* **1996**, *5−6*, 1003. [12d] J.-Y. Niu, B.-Z. Shan, X.-Z. You, H.-K. Fan, B.-C. Yip, *Transition Met. Chem.* **1999**, *24*, 108. [12e] J.-Y. Niu, J.-P. Wang, Y. Bo, D.-B. Dang, Z.-Z. Yuan, *J. Chem. Crystallogr.* **2000**, *30*, 43−48. [12f] H.-F. Fun, K. Chinnakali, B.-C. Yip, J.-Y. Niu, J.-P. Wang, X.-Z. You, *Acta Crystallogr., Sect. C* **1998**, *54*, 327.
[13] [13a] A. Mhanni, L. Ouahab, O. Pena, D. Grandjean, C. Garrigou-Lagrange, P. Delhaes, *Synth. Met.* **1991**, *41−43*, 1703. [13b] D. Attanasio, C. Bellitto, M. Bonamico, V. Fares, S. Patrizo, *Synth. Met.* **1991**, *41−43*, 2289. [13c] M. Clemente-León, E. Coronado, J.-M. Galán-Mascarós, C. Gimnéz-Saiz, C.-J. Gómez-García, T. Fernández-Otero, *J. Mater. Chem.* **1998**, *8*, 309.
[14] L. Ouahab, M. Bencharif, A. Mhanni, D. Pelloquin, J. F. Halet, O. Pena, J. Padiou, D. Grandjean, C. Garrigou-Lagrange, J. Amiell, P. Delhaes, *Chem. Mater.* **1992**, *4*, 666.
[15] A. Davidson, K. Boubekeur, A. Penicaud, P. Auban, C. Lenoir, P. Batail, G. Herve, *J. Chem. Soc., Chem. Commun.* **1989**, 1373.
[16] C. J. Gomez-Garcia, L. Ouahab, C. Gimenez-Saiz, S. Triki, E. Coronado, P. Delhaes, *Angew. Chem. Int. Ed. Engl.* **1994**, *33*, 223.
[17] C. J. Gomez-Garcia, C. Gimenez-Saiz, S. Triki, E. Coronado, P. Le Magueres, L. Ouahab, L. Ducasse, C. Sourisseau, P. Delhaes, *Inorg. Chem.* **1995**, *34*, 4139−4151.
[18] C. J. Gomez-Garcia, C. Gimenez-Saiz, S. Triki, E. Coronado, L. Ducasse, P. Le Magueres, L. Ouahab, P. Delhaes, *Synth. Met.* **1995**, *70*, 783.
[19] O_a refers to oxygen atoms connecting the P and Mo atoms; O_b refers to oxygen atoms located in the shared corners between two Mo_3O_{13} units; O_c refers to oxygen atoms connecting edge-sharing MoO_6 octahedra in the Mo_3O_{13} units; O_t are the terminal oxygen atoms.
[20] J. R. Galan-Mascaros, C. Gimenez-Saiz, S. Triki, C. J. Gomez-Garcia, E. Coronado, L. Ouahab, *Angew. Chem. Int. Ed. Engl.* **1995**, *24*, 1460.
[21] H. T. Evans, T. J. R. Weakey, G. B. Jameson, *J. Chem. Soc., Dalton Trans.* **1996**, 2573.
[22] B. B. Yan, Y. Xu, X. H. Bu, N. K. Goh, L. S. Chia, G. D. Stucky, *J. Chem. Soc., Dalton Trans.* **2001**, 2009−2014.
[23] J.-P. Wang, Q. Wu, J.-Y. Niu, *Sci. China, Ser. B* **2002**, *3*, 210−217.
[24] C. H. Evans, *Biochemistry of Lanthanides*, Plenum, New York, **1990**, p 47.
[25] F. H. Spedding, in *Kirk-Othmer Encyclopedia of Chemical Technology*, 3rd ed. (Eds.: M. Grayson, D. Eckroth), Wiley, New York, **1982**, vol. 19, p. 883.
[26] *Lanthanide Probes in Life, Chemical and Earth Sciences* (Eds.: J. C. G. Bünzli, G. R. Choppin), Elsevier, Amsterdam, **1989**.
[27] C. Lescop, E. Belorizky, D. Luneau, P. Rey, *Inorg. Chem.* **2002**, *41*, 3375−3384.
[28] I. A. Setyawati, S. Liu, S. J. Rettig, C. Orvig, *Inorg. Chem.* **2000**, *39*, 496−507.
[29] J. H. Melman, C. Rohde, T. J. Emge, J. G. Brennan, *Inorg. Chem.* **2002**, *41*, 28−33.
[30] R. D. Claude, F. Michael, F. Raymonde, T. Rene, *Inorg. Chem.* **1983**, *22*, 207−216.
[31] J.-Y. Niu, J.-P. Wang, L.-Q. Ma, *Chin. Sci. Bull.* **1996**, *41*, 328 (in Chinese).
[32] C. Sanchez, J. Livage, J. P. Launay, M. Fournier, Y. Jeannin, *J. Am. Chem. Soc.* **1982**, *104*, 3194−3202.
[33] J. N. Barrows, M. T. Pope, *Adv. Chem. Ser.* **1990**, *226*, 403.
[34] R. D. Peacock, T. J. R. Weakley, *J. Chem. Soc., A* **1971**, 1836−1839.
[35] N. Haraguchi, Y. Okaue, T. Isobe, Y. Matsuda, *Inorg. Chem.* **1994**, *33*, 1015−1020.
[36] M. R. Antonio, L. Soderholm, C. W. Williams, N. Ullah, L. C. Francesconi, *J. Chem. Soc., Dalton Trans.* **1999**, 3825−3830.
[37] G. M. Sheldrick, *SHELXTL-97, Program for the Refinement of Crystal Structures*, University of Göttingen, Germany, **1997**.

Received January 24, 2003
Early View Article
Published Online October 23, 2003

